



### **Science Arts & Métiers (SAM)**

is an open access repository that collects the work of Arts et Métiers Institute of Technology researchers and makes it freely available over the web where possible.

This is an author-deposited version published in: <https://sam.ensam.eu>  
Handle ID: <http://hdl.handle.net/10985/9963>

#### **To cite this version :**

Shaoxiong LIANG, Papa-Birame GNING, Laurent GUILLAUMAT - Quasi-static behaviour and damage assessment of flax/epoxy composites - Materials and Design - Vol. 67, p.344-353 - 2015

Any correspondence concerning this service should be sent to the repository

Administrator : [scienceouverte@ensam.eu](mailto:scienceouverte@ensam.eu)



# Quasi-static behaviour and damage assessment of flax/epoxy composites

Shaoxiong Liang<sup>a,b,\*</sup>, Papa-Birame Gning<sup>a</sup>, Laurent Guillaumat<sup>b</sup>

<sup>a</sup> DRIVE-ISAT, Université de Bourgogne, 58027 Nevers Cedex, France

<sup>b</sup> LAMPA, Arts et Métiers ParisTech, 49100 Angers Cedex, France

## A B S T R A C T

Experimental investigations were conducted on flax and E-glass fibres reinforced epoxy matrix composites subjected to quasi-static loadings. Flax/epoxy samples having  $[0]_{12}$ ,  $[90]_{12}$ ,  $[0/90]_{3S}$  and  $[\pm 45]_{3S}$  stacking sequences, with a fibre volume fraction of 43% have been tested under tension, compression and in-plane shear loadings. Overall, the compression strength of glass/epoxy was 76% greater than for the flax/epoxy composite. The damage evolution of flax/epoxy of  $[0/90]_{3S}$  and  $[\pm 45]_{3S}$  samples has been evaluated in terms of transverse crack densities with respect to the load increment. The crack density exhibited a classical “S” shaped pattern for  $[0/90]_{3S}$  and linearly for  $[\pm 45]_{3S}$  specimens versus the applied load. The final crack densities were respectively of 32/cm and 25/cm for the  $[0/90]_{3S}$  and  $[\pm 45]_{3S}$  samples.

### Keywords:

Flax fibres

E-glass fibres

Polymer-matrix composites

Mechanical properties

Damage mechanics

## 1. Introduction

With the environmental concerns, vegetal fibre reinforced polymer composites are increasingly considered as valid alternatives to conventional glass composites for mass production of composite materials [1]. Natural fibres offer various advantages compared to conventional man-made fibres and their processing requires low energy consumption and production costs [2]. Fibres are extracted from renewable and biodegradable resources and some varieties can offer specific properties, comparable to those of glass fibre. In particular, flax fibres extracted from an abundant and local resource in Europe, are known to have interesting mechanical properties as mentioned in the literature [3,4]. It emerged from the review that most of the available mechanical properties involving continuous Flax Fibre Reinforced Polymer (FFRP) composites are often limited to tensile data on unidirectional (UD) laminates loaded along the fibre direction [5,7]. However, most composite structures have multidirectional stacking sequences, and their compression and shear properties also need to be known. Therefore, the present work deals with the characterization of the quasi-static tensile, compression and in-plane shear properties of flax/epoxy. Several stacking sequences have been investigated:  $[0]_{12}$ ,  $[90]_{12}$  and  $[0/90]_{3S}$ , respectively noticed as FE\_0, FE\_90 and FE\_090 specimens. Flax laminate of  $[\pm 45]_{3S}$ , (FE\_45), was dedicated to characterise the in-plane shear properties. The properties of

FE\_090 and FE\_45 have been compared to E-glass fibre reinforced epoxy (GE) composites having similar stacking sequence (noticed GE\_090 and GE\_45) and fibre volume fraction.

Damage assessment is an important issue in the performance of composite materials. The different damage mechanisms occurring for general Synthetic Fibre Reinforced Polymer (SFRP) specimens subjected to tensile loading are well-identified, i.e. fibre breakage, matrix crack, fibre/matrix interfacial debonding and delamination [17]. Recently developed FFRP present similar damage mechanisms. Liu and Hughes [18] have investigated the fracture toughness of flax fabric reinforced epoxy composites. The main failure modes observed were debonding of fibres from the matrix and brittle fracture of matrix. Nevertheless, the most common damage causing stiffness decrease for cross-ply laminates in tension load was the intra-laminar transverse matrix cracking occurring in  $90^\circ$  layers [19]. For examples, authors [20,21] have measured an average crack density (CD) of 7–38/cm for glass fibre reinforced composite, whereas Ogihara et al. [22] measured 3 to 20/cm for carbon/epoxy layers having different stacking orientations. As to FFRP, our previous studies [9] have highlighted that the crack density exhibits a two-stage and three-stage evolution as a function of the life ratio for  $[0/90]_{3S}$ , and  $[\pm 45]_{3S}$ , respectively.

In the present study, monotonic tensile loading up to failure and interrupted tensile test up to certain loading levels have been investigated in  $[0/90]_{3S}$  and  $[\pm 45]_{3S}$  flax/epoxy (FE) specimens. Material degradation modes and damage evolution have been assessed by observation of the fractured edges under a Scanning Electron Microscope (SEM) and the internal crack using an Optical Microscope (OM).

\* Corresponding author at: LAMPA, Arts et Métiers ParisTech, 49100 Angers Cedex, France. Tel.: +33 2 41 20 73 59.

E-mail address: [shaoxiong.liang@ensam.eu](mailto:shaoxiong.liang@ensam.eu) (S. Liang).

**Table 1**  
Properties of flax/epoxy and glass/epoxy composites. Standard deviations are given in brackets.

Notation	Fibre	Fabric	$m_{area}$ (g/m <sup>2</sup> )	Stacking sequence	$V_f$ (%)	$V_p$ (%)	$\rho_c$ (kg/m <sup>3</sup> )	$t$ (mm)
FE_0	Hermès	UD	140 (6)	[0] <sub>12</sub>	43.9	0.48	1310 (10)	2.55
FE_90	flax			[90] <sub>12</sub>	(1.5)	(0.02)		(0.12)
FE_090		Non- crimp	235 (16)	[0/90] <sub>3S</sub>	43.1	3.1	1280 (10)	2.18
FE_45				[±45] <sub>3S</sub>	(0.6)	(0.3)		(0.07)
GE_090	E-glass	Non- crimp	430 (5)	[0/90] <sub>3S</sub>	42.5	5.9	1730 (30)	2.33
GE_45				[±45] <sub>3S</sub>	(1.0)	(2.2)		(0.04)

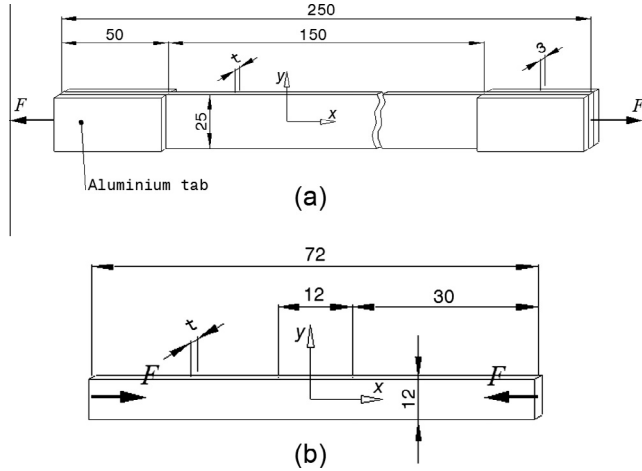


**Fig. 1.** Geometry of (a) tensile and in-plane shear and (b) compression specimens. Dimensions are given in mm.

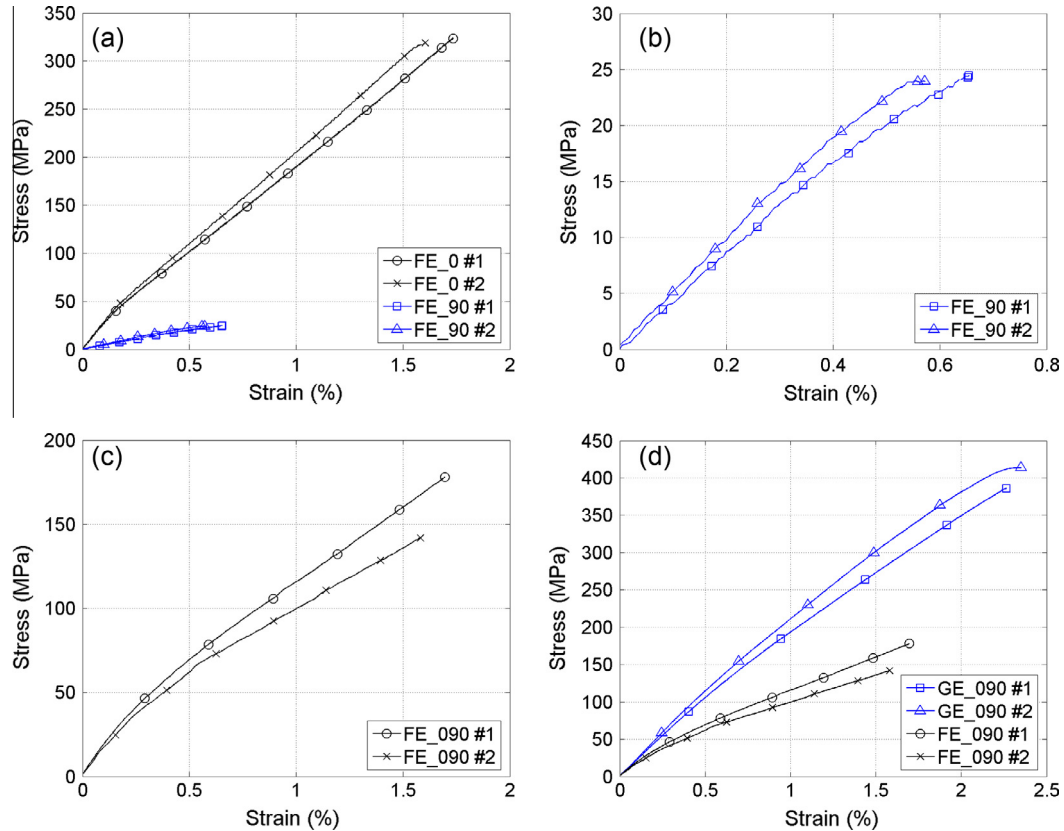


**Fig. 2.** Typical tensile stress-strain curves of (a) FE\_0, (b) FE\_90, (c) FE\_090 and (d) GE\_090 specimens.

## 2. Experimental methods

### 2.1. Materials

Flax/epoxy (FE) and E-glass/epoxy (GE) composites were made from dry reels of UD or balanced non-crimp fabrics. All fabrics were used as received without any further treatment. Composite layers were hand-laid up after being impregnated with an epoxy matrix system SR 8200/SD 8205 supplied by Sicomin. The matrix density was of 1.14 kg/m<sup>3</sup> at 20 °C and the measured glass transition temperature ( $T_g$ ) was 88 °C [6]. Laminates were cured under pressure between two heating plates. The temperature was constant at 60 °C for 8 h. The exhaustive parameters of the constituents and the fabrication process are given in [8,9]. The composite plates were then cut with a high-speed abrasive disc. Specimen notation, stacking sequences, fibre ( $V_f$ ) and porosity ( $V_p$ ) volume fractions, densities ( $\rho_c$ ) and thicknesses ( $t$ ) are given in Table 1. Comparable  $V_f$  of around 43% were measured for all composite types according the Method II of the standard ASTM: D 3171-11. This method consists of measuring the reinforcement quantity in the composite materials and the final composite thickness ( $t$  in mm). The fibre mass is calculated by the dry fabric areal weight ( $m_{area}$  in g/m<sup>2</sup>) multiplied by the number of plies ( $n$ ). The fibre volume fraction is calculated by Eq. (1). Where  $\rho_f$  is the fibre density and equal to 1500 kg/m<sup>3</sup> for flax fibre and 2600 kg/m<sup>3</sup> for glass ones.

$$V_f = \frac{n \times m_{area}}{\rho_f \times t} \quad (1)$$

### 2.2. Specimens and experimental measurements

The tensile properties of all specimens have been determined by quasi-static tests according to ISO 527-4 [23] standard on

**Table 2**

Mechanical properties of FE and GE composites. Standard deviations are given in brackets.

	$E_x^+$ (GPa)	$\nu_{xy}$	$\sigma_x^{UTS}$ (MPa)	$\varepsilon_x^{UTS}$ (%)	$E_x^-$ (GPa)	$\sigma_x^{UCS}$ (MPa)	$\varepsilon_x^{UCS}$ (%)	$G_{12}$ (GPa)	$\tau_{12}^{USS}$ (MPa)	$\gamma_{12}^{USS}$ (%)
FE_0	22.8 (1.0)	0.434 (0.084)	318 (12)	1.65 (0.05)	24.7 (0.6)	136 (2)	2.41 (0.27)	–	–	–
FE_90	4.52 (0.18)	0.084 (0.011)	26.1 (0.6)	0.622 (0.036)	5.93 (0.27)	100 (4)	3.27 (0.12)	–	–	–
FE_090	14.5 (0.8)	0.153 (0.045)	170 (20)	1.72 (0.13)	13.0 (1.2)	98 (7)	2.12 (0.20)	–	–	–
FE_45	6.48 (0.66)	0.748 (0.035)	79.5 (6.6)	3.85 (0.62)	–	–	–	1.96 (0.17)	39.7 (3.3)	6.23 (1.08)
GE_090	21.9 (1.1)	0.142 (0.004)	380 (26)	2.16 (0.16)	27.3 (2.1)	405 (16)	1.63 (0.11)	–	–	–
GE_45	11.1 (1.1)	0.483 (0.083)	103 (8)	16.1 (2.1)	–	–	–	3.44 (0.26)	51.4 (4.2)	23.84 (3.17)

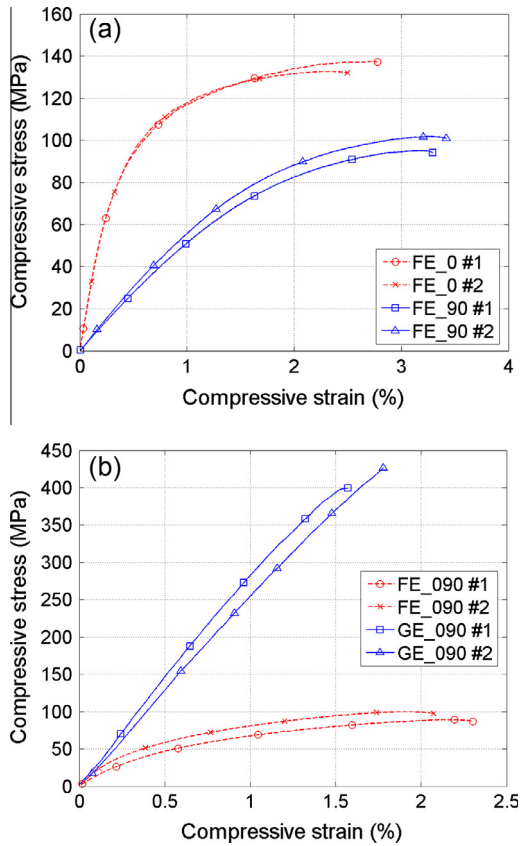


**Fig. 3.** Typical compression stress–strain curves of (a) FE\_0 and FE\_90, (b) FE\_090 and GE\_090 specimens.

rectangular shaped coupons. Specimens were equipped with aluminium end-tabs (Fig. 1a).  $x$  and  $y$  axis were designated as the axial and in-plane perpendicular directions respectively. Strain gauge rosettes (two perpendicular directions) were bonded on the middle of the surface of specimens for the strain measurement. Compression tests were conducted on  $[0]_{12}$ ,  $[90]_{12}$  and  $[0/90]_{3S}$  flax/epoxy composites and  $[0/90]_{3S}$  glass/epoxy specimens using a testing device similar to ISO 14126 [24] setup. The specimens of 72 mm long and 12 mm wide, without tabs, were rigidly clamped at their ends over 30 mm, leaving a short gauge length of 12 mm, to prevent buckling (Fig. 1b). Two longitudinal strain gauges were glued to the centre of the front and back faces of the specimens.

All the in-plane shear specimens (Fig. 1a) were cut on  $[\pm 45]_{3S}$  laminates (FE\_45 and GE\_45) according to ISO 14129 [25]. The shear stress ( $\tau_{12}$ ) was evaluated by Eq. (2) where  $F$ ,  $b$  and  $t$  stand for the applied force, the width and the thickness of the specimen, respectively. Subscripts 1 and 2 refer to the longitudinal and transversal directions of the fibres, respectively. The shear strain ( $\gamma_{12}$ ) was calculated using Eq. (3).  $\varepsilon_{xx}$  and  $\varepsilon_{yy}$  were strains recorded from

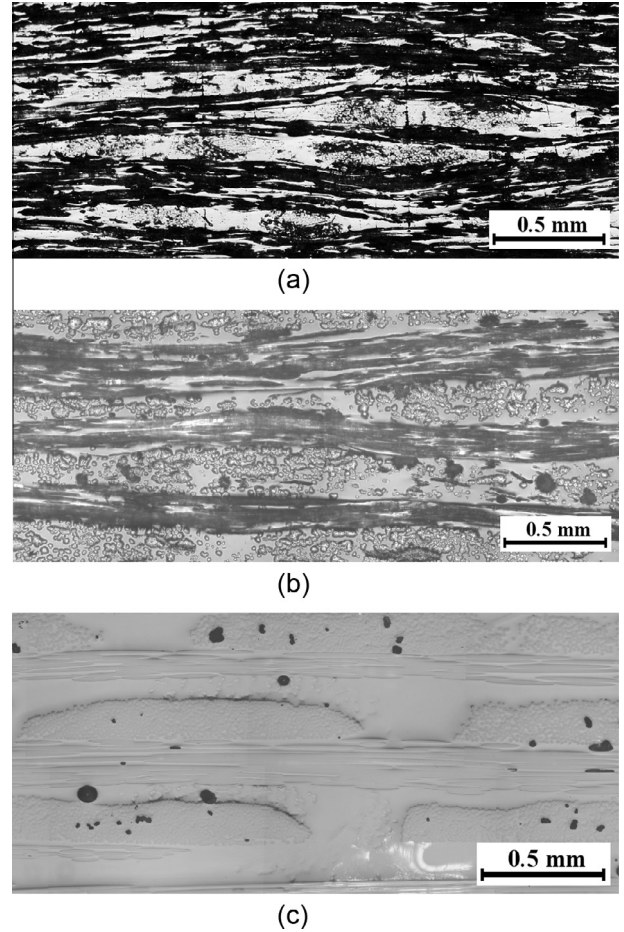


**Fig. 4.** Micrographs of fibre alignment for: (a) FE\_0, (b) FE\_090 and (c) GE\_090 specimens.

strain gauge rosettes, along the loading direction and its in-plane perpendicular direction.

$$\tau_{12} = \frac{F}{2bt} \quad (2)$$

$$\gamma_{12} = \varepsilon_{xx} - \varepsilon_{yy} \quad (3)$$

The above monotonic tests have been carried out up to failure, with five repetitions for each loading case to assess the variability of the material properties.

### 2.3. Interrupted tensile test procedures

$[0/90]_{3S}$  and  $[\pm 45]_{3S}$  tensile specimens reinforced with flax fibres were subjected to interrupted tensile loadings. The cross-head speed was 2 mm/min and the different loading levels were: 40%, 60%, 80% and 100% of the Ultimate Tensile Stress (UTS)

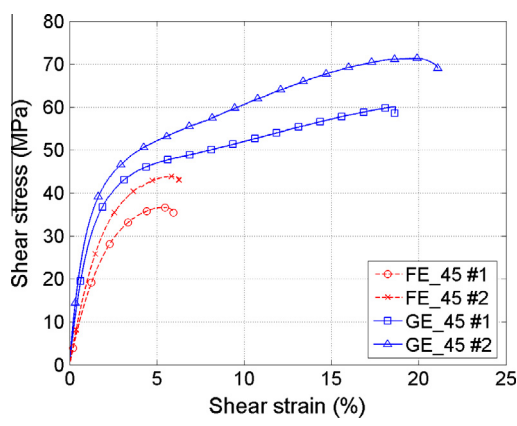


Fig. 5. Typical in-plane shear stress–strain curves of FE\_45 and GE\_45 specimens.

measured in the previous tensile and in-plane shear tests. These tests were doubled for each level. Then the specimens were cut and polished to observe the transverse crack density evolution.

All the mechanical experiments were performed on an MTS 809 servo-hydraulic testing machine having a capacity of 100 kN at the constant temperature of 23°, without humidity control.

## 2.4. Damage observations

Microscopic observations have been performed on the tested specimens in order to assess the damage modes and their development. An Axiovert Optical Microscope (OM) was used for the optical observation. Specimens' fractured edges were coated with a thin layer of gold and examined with a Zeiss Supra 25 Scanning Electron Microscope (SEM).

## 3. Results and discussion

### 3.1. Tensile behaviour

Plots of the lowest and the highest tensile response of flax/epoxy and glass/epoxy specimens are shown in Fig. 2. The stress is plotted as a function of the axial strain ( $\epsilon_{xx}$ ). The curves of the FE\_0 specimen showed a change of slope at the knee-point occurring for  $\epsilon_{xx}$  between 0.2% and 0.3%, after an initial linear stage, followed by a quite linear second stage up to failure (Fig. 2a). This phenomenon, attributed to the nonlinear behaviour of the reinforcement, has been reported in the literature for continuous FFRP composites [16]. FE\_90 specimens for which all fibres were oriented perpendicularly to the loading direction exhibited a

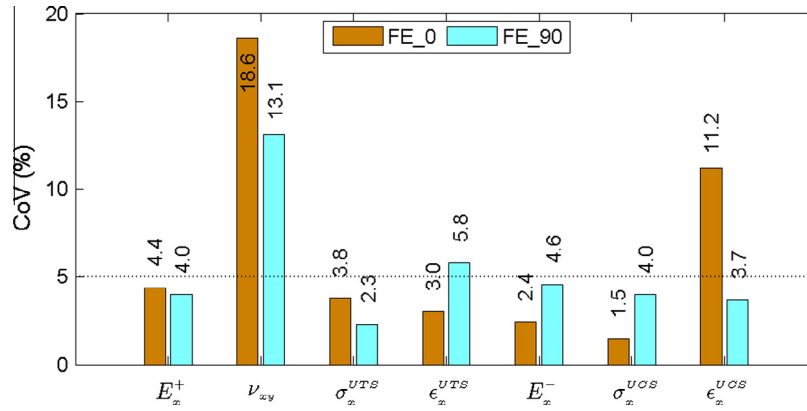


Fig. 6. CoV of mechanical properties of FE\_0 and FE\_90.

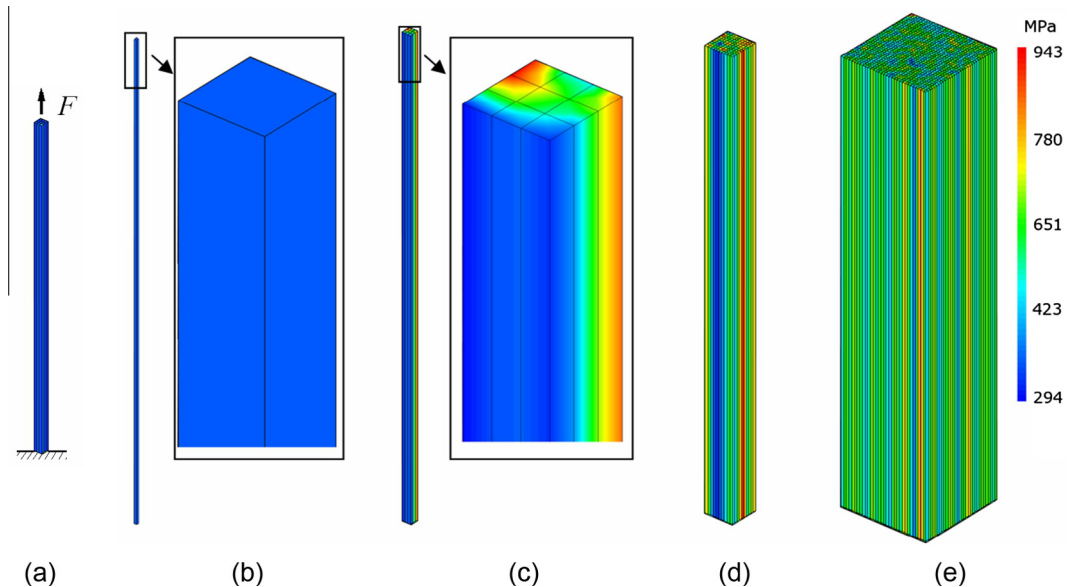
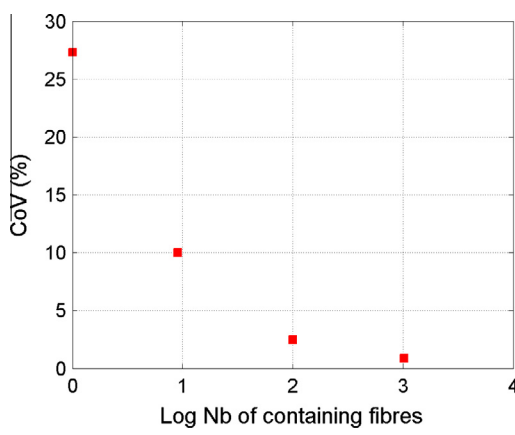


Fig. 7. FEM of fibres' variability: (a) boundary conditions and loading, models of bundles containing: (b) 1 single fibre, (c) 9 fibres, (d) 100 fibres and (e) 1024 fibres.





**Fig. 8.** CoV of bundles' modulus as a function of the number of fibres contained in bundles.

quasi-linear response (Fig. 2b). The specimen fracture occurred at  $\epsilon_{xx} = 0.62\%$  on average, slightly higher than for flax/polyester with a  $V_f = 21\%$  reported by Baley et al. [13]:  $\epsilon_{xx} = 0.44\%$ . However, this result is in accordance with the maximum transverse strain of 0.2–0.7% for conventional synthetic fibre based composites as reported in [11].

For  $[0/90]_{3S}$  specimens, the tensile curves of GE\_090 were relatively straight, with a barely visible knee-point at around  $\epsilon_{xx} = 0.5\%$  (Fig. 2 d). This knee-point is generally due to the development of cracks in the  $90^\circ$  oriented layers. Therefore FE\_090 samples seemed to present 2 knee-points (Fig. 2c). The first occurring at  $\epsilon_{xx} = 0.2$ – $0.3\%$ , corresponding to the slope changing point of the  $0^\circ$  flax layers as seen for FE\_0 specimens. The second one happening at  $\epsilon_{xx} = 0.5$ – $0.6\%$ , was attributed to the failure of the  $90^\circ$  plies. It worth to noted that, for the specimen FE\_090 #1 in Fig. 2c, the second knee point is much less marked than that in the FE\_090 #2 curve. This could be explained by the fact that the strain gauge is small (5 mm in length), the transverse crack may start randomly, far away from the measured area.

All the experimental elastic and ultimate properties of the composites determined from tensile tests are listed in Table 2. The superscripts +, –, UTS, UCS and USS refer to tension or compression loading, ultimate tensile, compression and shear stresses respectively. It can be noticed that the longitudinal Young's modulus ( $E_x^+$ ), ultimate stress ( $\sigma_x^{UTS}$ ) and strain ( $\epsilon_x^{UTS}$ ) of FE samples are consistent with the experimental data given in [5–7]. Although the  $[\pm 45]_{3S}$  specimens were dedicated to in-plane shear properties

assessment. Their tensile properties were also estimated according to the ISO 527-4 [23] standard.

### 3.2. Compression properties

Typical compression stress–strain curves of flax and glass reinforced epoxy specimens are plotted in Fig. 3. FE samples exhibited nonlinear behaviour, whatever the fibre orientation (FE\_0, FE\_90 and FE\_090), suggesting collapse by buckling prior to material failure. Conversely, GE\_090 specimens exhibited linear response until failure.

Micrographs of the cross-sections of untested specimens revealed that flax fibres were not straight and presented some waviness, whereas glass fibres were perfectly straight and parallel to the specimen axes (Fig. 4). Therefore, the initial waviness of the flax reinforcement can initiate premature micro-buckling of the specimen [28].

The compression properties of FE and GE composites are given in Table 2. It appears that the compression strength of FE\_0 and FE\_090 composites are respectively 57% and 42% lower than in tension loading (Table 2). The fact that the ultimate compression properties become significantly lower than tensile ones can be explained by the lower inherent compressive properties of flax fibres as reported by Bos et al. [3]. The premature buckling due to fibre alignment defaults i.e. the waviness of fibres (Fig. 4b) also has an influence. Conversely, GE specimens exhibit better compression properties. A similar remark is also reported in [12] for glass/polyester.

### 3.3. In-plane shear properties

The shear stress–strain curves of FE\_45 and GE\_45 specimens are plotted in Fig. 5. For  $[\pm 45]_{3S}$  laminates, the influence of the matrix on the behaviour leads to a pronounced nonlinear stage before failure. The measured properties according to ISO 527-4 [23] and 14129 standards are presented in Table 2. As recommended in ISO 14129 [25], the reported ultimate shear stress ( $\tau_{12}^{USS}$ ) corresponds to  $\gamma_{12} = 5\%$ , as the ultimate shear strain was higher than that level. Overall, the GE\_45 was respectively 43% and 23% higher than the FE\_45 in terms of shear modulus and strength.

Throughout tests, GE composites exhibited higher properties under tensile, compression and in-plane shear loadings (Table 2). However, the lower density of FE composites compared to GE composites (Table 1) reduced the differences in terms of specific

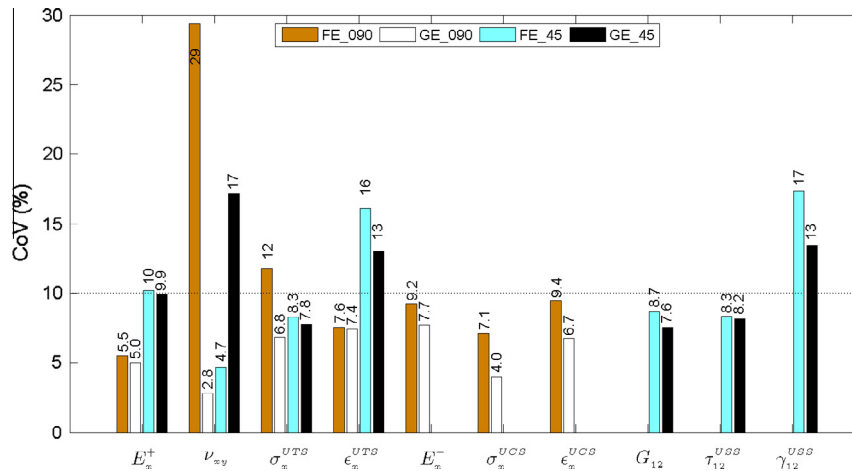


**Fig. 9.** CoV of mechanical properties of FE\_090, GE\_090, FE\_45 and GE\_45.

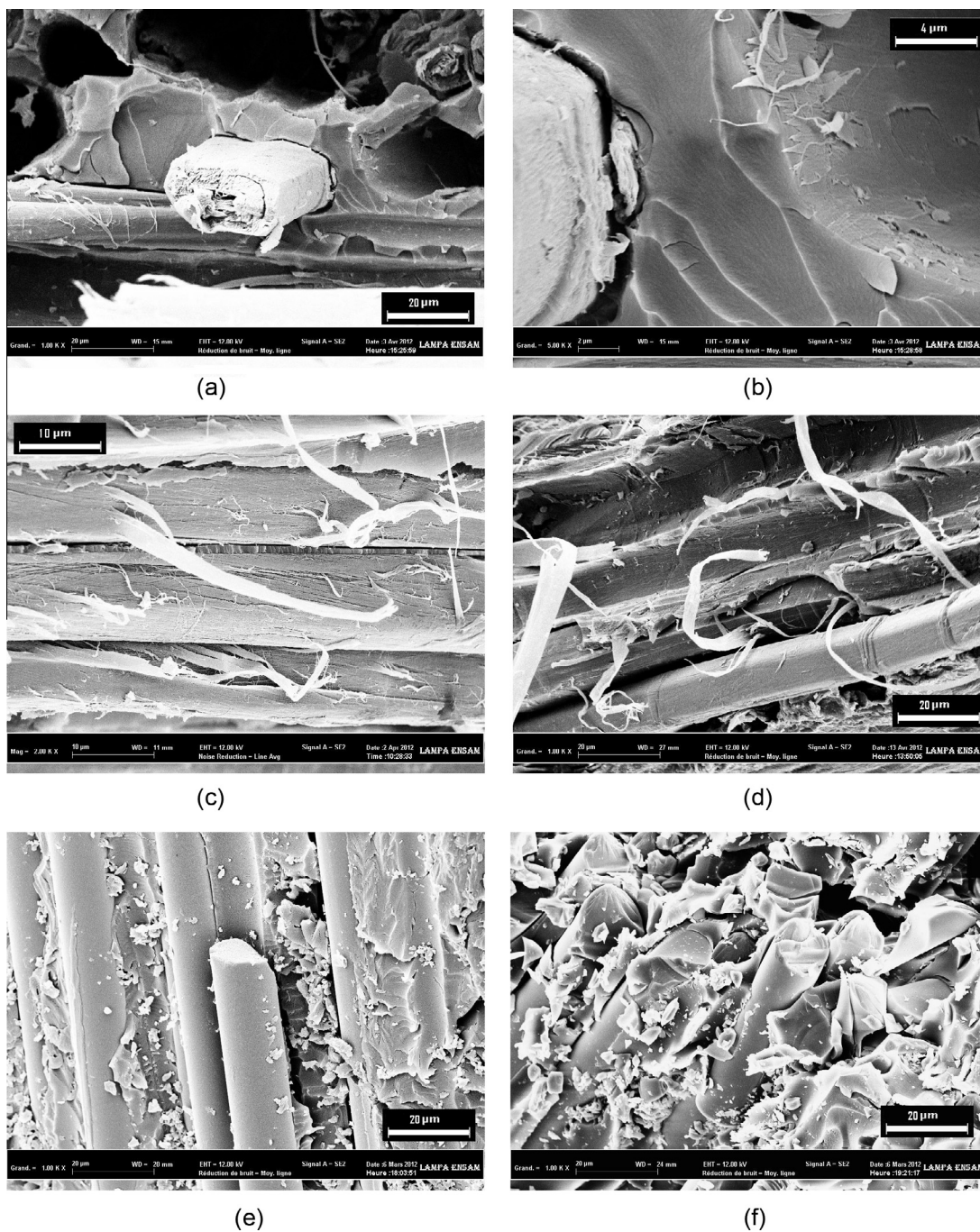


**Fig. 10.** SEM images of the edges of fractured specimens: (a) pulled-out flax fibre and imprints of removed fibres in the 0° layer, (b) detail view of flax fibre/matrix interface and pull-out imprint, (c) view of denuded fibres in fractured 90° oriented layer, (d) denuded flax fibres and removed fibre prints in matrix of 45° oriented layers, (e) matrix residues on the fibre surface of failed glass/epoxy interface of GE\_090 specimen and (f) glass fibres enclosed in epoxy matrix of GE\_45 sample.

properties. Depending on properties, the gaps between the two materials that were in the range of 23% for the in-plane shear strength ( $\tau_{12}^{USS}$ ) and 76% for compression strength ( $\sigma_x^{UCS}$ ), decreased to -4% for the specific in-plane shear strength and 67% for the specific compression strength. It can be highlighted that the specific in-plane shear strength of flax/epoxy is 4% higher than that of glass/epoxy. However, this advantage can be mitigated when we consider the scattering of the property by its standard deviation and the limited number of repetitions.

It is commonly reported in the literature [14,15], that the specific properties of elementary flax fibres ( $\rho_{flax} = 1500 \text{ kg/m}^3$ ) are higher than those of E-glass fibres ( $\rho_{glass} = 2600 \text{ kg/m}^3$ ), due to

the difference of density of 42%. However, the important matrix volume fraction of around 57% decreases the difference of density between FE and GE composites to only 26% (Table 1). Thus, the specific properties of flax fibre reinforced composites remain generally lower than that of glass fibre reinforced ones.

### 3.4. Variability of mechanical properties

Flax fibres, as well as other natural fibres, present important scattering of geometrical, mechanical and chemical properties. According to authors ([3,4]), the Coefficient of Variation (CoV), defined as the standard deviation divided by the mean value, of



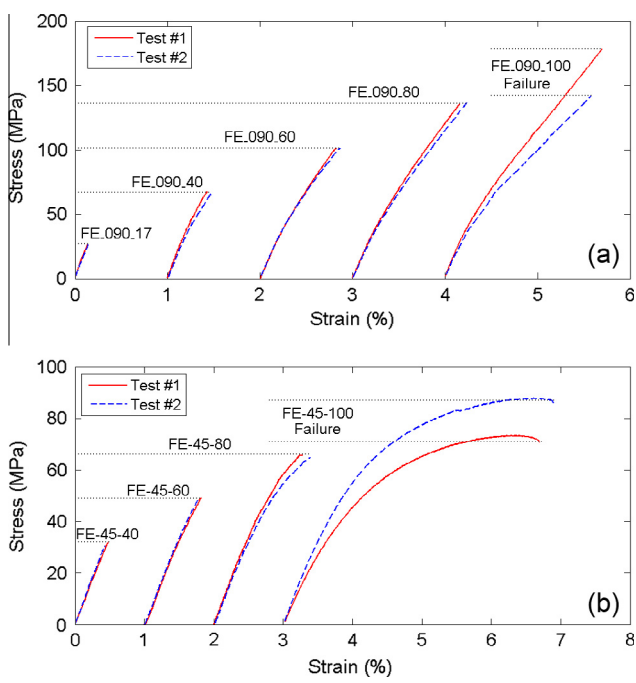


**Fig. 11.** Stress-strain curves of interrupted tensile tests for: (a) FE\_090 and (b) FE\_45 specimens.

the mechanical properties of elementary flax fibres, is between 21% and 57%. In this present study, the measured CoV of the properties of the flax/epoxy UD layers are generally lower than 5%, except for Poisson's ratios ( $\nu_{xy}$ ), ultimate tensile strain ( $\epsilon_x^{UTS}$ ) for FE\_90 and compression strain ( $\epsilon_{11}^{UCS}$ ) for FE\_0, as illustrated in Fig. 6. This remark highlights the fact that the variability level of UD flax composites' properties is largely smaller than that of single fibres. The decrease of scattering from the single fibre scale to the composite specimen scale can be explained by an "averaging" effect due to the very large number of single fibres contained in the composite sample. Indeed, under load, the reaction of fibres having higher mechanical properties compensates that of weaker ones, covering the dispersions of behaviours between them. This results in the decrease of the macroscopic variability at laminate scale.

To illustrate this effect, a Finite Element Model (FEM) of a single fibre and bundles of fibres loaded in tension, was achieved with *Cast3m* code, in order to estimate the variability of the bundle's Young's modulus as a function of the number of considered fibres. The 3D model is constructed by 8 nodes cubic elements. Four models containing  $n_f$  fibres, respectively equal to 1, 9, 100 and 1024 (Fig. 7), were longitudinally loaded with an uniaxial tensile force  $F$  applied on top of the fibres bundles and rigidly fixed at the other extremity (Fig. 7a). The input of longitudinal modulus of each fibre was randomly affected following a normal distribution law with a CoV of 28% taken from Baley's study [4]. The bundle's modulus ( $E$ ) was calculated by Eq. (4), where  $S$  and  $\epsilon$  are respectively the cross-section area and the longitudinal strain of the bundle.

$$E = \frac{F}{S \cdot \epsilon} \quad (4)$$

The CoV of each bundle was determined after 50 random simulations and plotted in Fig. 8. It appeared clearly that, the scattering decreased very strongly with the number of fibres and was lower than 1% for  $n_f = 1024$ . By extrapolation, it is possible to imagine that the CoV of a full scale specimen that contains a very large number of fibres should be insignificant compared to the variability of a single fibre's properties. However, some following reasons can slow down

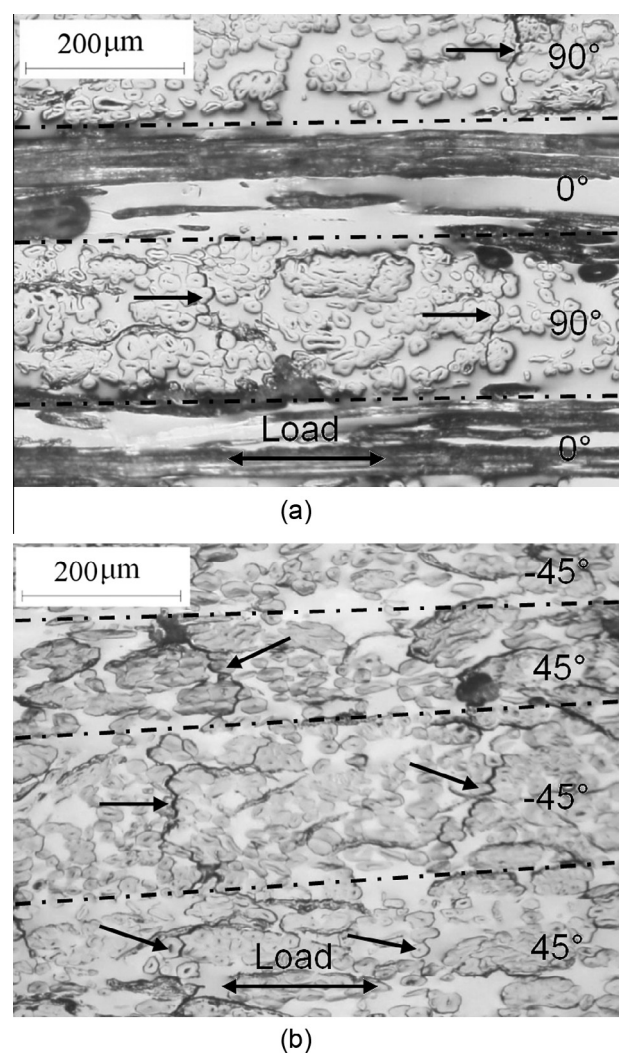


**Fig. 12.** OM images of (a) FE\_090 and (b) FE\_45 specimens tested at 80% UTS. Arrows point to the through-the-thickness cracks. Layers orientation and loading direction are indicated.

this trend and explain why the experimental CoV measured are higher. The FEM did not consider other morphological, mechanical variabilities or defects induced by the process that may possibly interact and influence the results. The fibres were considered geometrically perfect and neither the matrix, nor the interfaces have been modelled. In addition, other sources of dispersion can come from the heterogeneity of constituents, fibres' misalignment and waviness, the uncertainties of measurements, etc.

In the same manner, the measured CoV of the properties of the flax/epoxy UD layers were on general lower than that of flax/epoxy cross-ply laminates (FE\_090 and FE\_45). For the latter the CoV were globally beneath 10%, except for the Poisson's ratio ( $\nu_{xy}$ ) for FE\_090, ultimate tensile strength  $\sigma_x^{UTS}$  for FE\_090, ultimate tensile and shear strain ( $\epsilon_x^{UTS}$  and  $\gamma_{12}^{USS}$ ) for FE\_45, as shown in Fig. 9. The increase of the properties' scattering, from UD to cross-ply laminate, can be explained by the presence of half less fibres loaded, hence less "averaging" effect, and the existence of a second stacking direction that adds the origins of uncertainties. It is remarkable that the variability of flax/epoxy laminates (FE\_090 and FE\_45) was of the same level as that of man-made E-glass/epoxy laminates (GE\_090 and GE\_45) (Fig. 9). As illustrated by the 3D FEM, the scattering of constitutive elementary fibres is covered by the averaging effect in laminate scale. Thus, disregard the important variation in



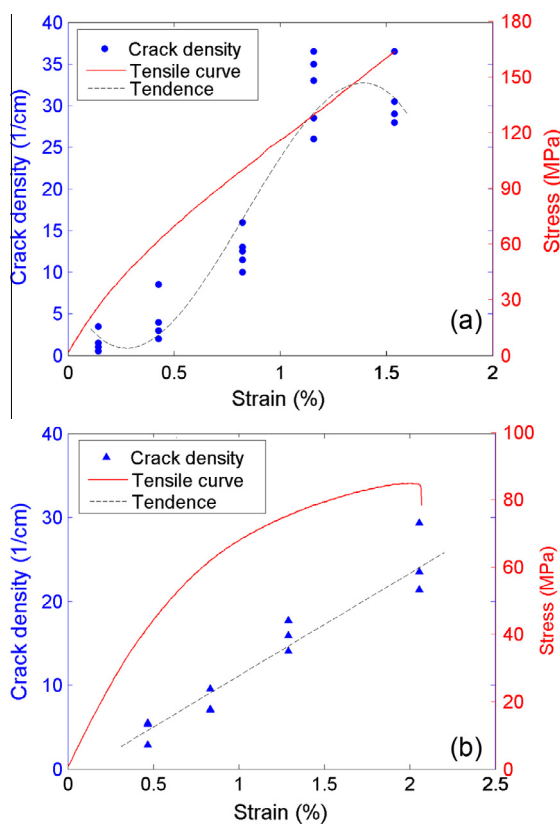


**Fig. 13.** Crack density and tensile stress as a function of longitudinal strain for: (a) FE\_090 and (b) FE\_45 specimens.

the properties of vegetal fibre, the CoV of composites reinforced by flax fibre and by glass fibre exhibit comparative dispersion. This remark can be also observed in other studies [2,8,16]. It is thought that the scattering in composite scale is more attributable to the uncertainties on manufacturing processes rather than CoV of the elementary fibres.

It worth to note that the Poisson's ratios have small average values (Table 2) and are very sensitive to fibre orientation. Therefore their CoV was relatively high. For comparison, the CoV of the Poisson's ratio of a glass/polyester composite reported in [12] is 29%.

### 3.5. Fracture analysis

Micrographics of fractured edges of tested FE\_090, FE\_45 and GE\_090 specimens in tensile loading until failure are shown in Fig. 10. Single fibres from pull-out and remaining traces of pulled fibres from the matrix were observed in 0° oriented layers of

FE\_090 specimens (Fig. 10a and b). Almost no matrix residue has been found on the surface of the fibres of 0°, 90° (Fig. 10a and c) and 45° (Fig. 10d) oriented layers. This observation is consistent with the poor adhesion between hydrophilic plant fibres and hydrophobic matrix as reported in [26]. By comparison with [0/90]<sub>3S</sub> and [±45]<sub>3S</sub> glass/epoxy specimens, matrix remnants were found attached to the surface of the fibre interface due to a stronger adhesion (Fig. 10e and f).

It can be noticed that, flax fragments were found stuck to the matrix after fibre pull-out (Fig. 10b). Moreover, superficial flax shavings appeared partially separated from the fibres, i.e. not completely torn from the reinforcements (Fig. 10c and d). The presence of flax residues on both matrix and fibre surfaces suggests that the adhesion between the primary and secondary fibre cell walls has comparable toughness to the primary cell wall/epoxy matrix interface. Therefore, fibre cell walls separation can be considered as an additional type of damage mechanism for vegetal fibre reinforced composites. Until now, no data of the primary/secondary cell walls interface resistance is available in literature. Further work is needed to measure this toughness knowing that the main difficulty is that the thickness of the primary cell walls, of approximately 0.2 µm, is very small [27].

### 3.6. Interrupted tensile tests

Stress/strain curves of FE\_090 and FE\_45 specimens under interrupted tensile loading are plotted in Fig. 11. Tests carried out to each peak stress were repeated once and plotted with an offset by 1% along the strain axis for clarity.

Curves of [0/90]<sub>3S</sub> flax/epoxy specimens tested at 60%, 80% and 100% UTS, respectively named FE\_090\_60, FE\_090\_80 and FE\_090\_100, exhibited one knee-point (Fig. 11a) as described earlier in Section 3.1. The FE\_090\_17 couple of curves (FE\_090 tested up to 17% UTS) is situated in the first linear stage before the knee-point, whereas FE\_090\_40 (FE\_090 tested up to 40% UTS) curves are situated between the two transition points (Fig. 11a). Regarding the tensile curves of FE\_45, a quasi-linear trend was noticed up to 60% UTS, then specimens went into nonlinear behaviour until breakage (Fig. 11b).

Samples tested at different load levels were then cut parallel to the loading direction for damage assessment in terms of crack density development. Fig. 12 shows micrographics of FE\_090 and FE\_45 samples loaded at 80% UTS. Cracks propagated tortuously only in 90° layers for [0/90]<sub>3S</sub> laminates (Fig. 12a) by following the fibre/matrix interface which is the lowest energy path. Similar cracks were observed in all plies of [±45]<sub>3S</sub> tested samples (Fig. 12b).

Correlation can be found between crack density (CD) and longitudinal stress in the superposition of both results as a function of tensile strain in Fig. 13. For FE\_090 specimens, the CD exhibited an "S" shaped profile corresponding to the development of cracks in the 90° layers until saturation. Indeed, moderate cracks

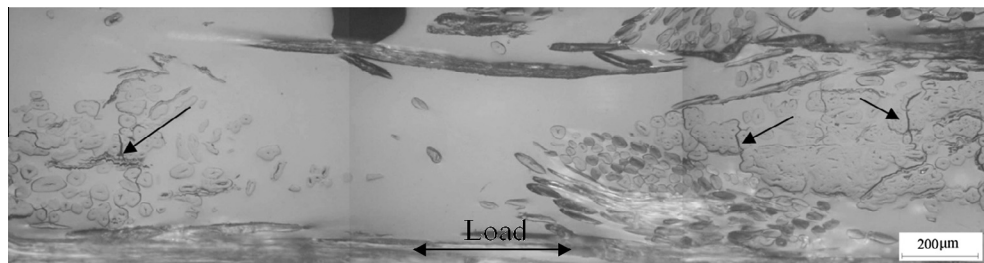


**Fig. 14.** OM images of transverse crack distribution and rich resin zones (monochrome areas) of an FE\_090 specimen loaded up to failure. Arrows point to the cracks.

appeared at 17% UTS (30 MPa) and 40% UTS (68 MPa) loading levels. Then, their number increased strongly at 80% UTS (136 MPa), corresponding to an average  $\varepsilon_{xx}$  of 1.15%. At that point, the longitudinal strain is higher than FE\_90 specimen's maximum tensile strain ( $\varepsilon_x^{UTS}$ ) of 0.62% (Table 2). The CD seemed to reach a saturation level of 30/cm on average and remained constant until failure. Comparatively, this density is respectively 1.5 to 3 times and 1 to 5 times higher than that of equivalent carbon/epoxy [22] and glass/epoxy [20,21] composites. There was no clear cause for the first knee-point occurring for  $\varepsilon_{xx}$  between 0.2% and 0.3%, because this phenomenon took place in 0° layers while the observed cracks were measured in the 90° plies.

For FE\_45 specimens, the CD exhibited a linear trend until breakage (Fig. 13b). The intersection of the abscissa with the linear extrapolation of the CD tendency curves is situated at strain higher than zero. This can be explained by the existence of an energy threshold for the cracking development. The dissimilarity of tendencies for these two composites can be explained by the stacking sequences because in the FE\_45, only 45° layers exist. While for FE\_090, the behaviour of 90° oriented layers depends on the matrix, the transverse properties of flax fibres and their interface adhesion, which are weaker than the properties of the longitudinal fibres. Therefore, cracks developed first in 90° layers and reached saturation level beyond which, the fibre breakage mode was then activated in 0° layers. As to FE\_45 samples, all layers were affected by the cracking and no switch of damage mechanism could occur.

The number of cracks increased with the load for both FE\_090 and FE\_45 specimens. The crack spacing was not regular, even for higher levels, when saturation was reached. Larger distances corresponded to rich resin zones, e.g. monochrome areas visible along the loading axis of a FE\_090 sample tested until failure in Fig. 14. In fact, the difference between the maximum tensile strain of the pure epoxy resin, in the range of 1.7–4.6% [10] and that of 90° oriented FFRP composites i.e. FE\_90 samples of 0.62%, suggests that the crack creation is probably due to the weakness of the transverse resistance of flax fibres or/and the poor interfacial adhesion properties between flax and matrix. Therefore, few cracks have been observed in resin rich zones. This observation reveals that, the increase of the mechanical properties of FFRP composites is linked to the improvement of the interfacial adhesion.

## 4. Conclusions

Experimental investigations of quasi-static tests (tension, compression and in-plane shear) have been conducted on [0]<sub>12</sub>, [90]<sub>12</sub>, [0/90]<sub>35</sub> and [±45]<sub>35</sub> flax/epoxy specimens and [0/90]<sub>35</sub> and [±45]<sub>35</sub> glass/epoxy specimens. Stress–strain curves of flax/epoxy exhibited nonlinear behaviour, when fibres were loaded along their axis. Knee-points were detected in the tensile curves at  $\varepsilon_{xx} = 0.2$ –0.3% due to the bilinear response of the fibres and at  $\varepsilon_{xx} = 0.5$ –0.6% corresponding to the failure of 90° layers. The initial undulation of flax fibres is supposed to be responsible for the nonlinear behaviour of FE composites under compression loading, because it favours micro-buckling. The comparison of FE and GE specimens having the same  $V_f$  and stacking sequences revealed maximum differences of 76% in compression strength, in favour of GE. However this difference has decreased to 67% for the specific compression strength due to the lower density of flax composite.

The material properties' variability was generally lower than 5% for UD FE and 10% for FE cross-ply laminates. The study shown that FFRP composites have the same scattering level of mechanical properties than conventional glass fibre reinforced polymer ones. The decrease of CoV from single fibre scale to the laminate one is explained by the averaging effect, which was illustrated via FEM simulations.

Microscope observations have revealed that the cell walls of fibres pull-out as a specific type of damage on flax/epoxy composites. The remains of the primary cell walls can be found attached both on the matrix and on the fibre, implying that the interface cohesion between fibre cell walls to be comparable to the flax fibre/epoxy interface one. Crack density quantification from interrupted tensile tests on FE\_090 specimens exhibited an “S” shape evolution with the strain. Beyond 80% UTS, saturation of the through-the-thickness cracking took place and the kinetics of damage changed from cracks in 90° layers to fibre breakage in 0° layers. As for FE\_45 specimens, the crack density increase depending on tensile strain was found linear until specimen failure, because +45° and –45° layers have the same behaviour and composite response is dominated by matrix behaviour.

## Acknowledgement

The financial support of the FABER fund from the Bourgogne Region, France is gratefully acknowledged.

## References

- [1] Corbière-Nicollier T, Gfeller Laban B, Lundquist L, Leterrier Y, Manson JAE, Joliet O. Life cycle assessment of biofibres replacing glass fibres as reinforcement in plastics. *Resour Conserv Recycl* 2001;33:267–87.
- [2] Bodros E, Pillin I, Montrelay N, Baley C. Could biopolymers reinforced by randomly scattered flax fibre be used in structural applications? *Compos Sci Technol* 2007;67:462–70.
- [3] Bos HL, Van Den Oever MJA, Peters OCJJ. Tensile and compressive properties of flax fibres for natural fibre reinforced composites. *J Mater Sci* 2002;37:1683–92.
- [4] Baley C. Analysis of the flax fibres tensile behaviour and analysis of the tensile stiffness increase. *Compos A* 2002;33:939–94.
- [5] Madsen B, Lilholt H. Physical and mechanical properties of unidirectional plant fibre composites – an evaluation of the influence of porosity. *Compos Sci Technol* 2003;63:1265–72.
- [6] Gning PB, Liang S, Guillaumat L, Pui WJ. Influence of process and test parameters on the mechanical properties of flax/epoxy composites using response surface methodology. *J Mater Sci* 2011;46:6801–11.
- [7] Assarar M, Scida M, Mahi AE, Poilâne C, Ayad R. Influence of water ageing on mechanical properties and damage events of two reinforced composite materials: flax fibres and glass fibres. *Mater Des* 2011;32:788–95.
- [8] Liang S, Gning PB, Guillaumat L. A comparative study of fatigue behaviour of flax/epoxy and glass/epoxy composites. *Compos Sci Technol* 2012;72(5):535–43.
- [9] Liang S, Gning PB, Guillaumat L. Properties evolution of flax/epoxy composites under fatigue loading. *Int J Fatigue* 2014;63:36–45.
- [10] Factsheet of SICOMIN, SR 8200 Systèmes époxydes de stratification. Version du 9 Janvier 2002.
- [11] Deng S, Ye L, Mai Y. Influence of fibre cross-sectional aspect ratio on mechanical properties of glass fibre/epoxy composites I. Tensile and flexure behaviour. *Compos Sci Technol* 1999;59:1331–9.
- [12] Zhou G, Davies GAO. Characterization of thick glass woven roving/polyester laminates: 1. tension, compression and shear. *Composites* 1995;26:579–86.
- [13] Baley C, Perrot Y, Busnel F, Guezennec H, Davies P. Transverse tensile behaviour of unidirectional plies reinforced with flax fibres. *Mater Lett* 2006;60:2984–7.
- [14] Velde KV, Kiekens P. Thermoplastic pultrusion of natural fibre reinforced composites. *Compos Struct* 2001;54:355–60.
- [15] Bodros E, Baley C. Study of the tensile properties of stinging nettle fibres (*Urtica dioica*). *Mater Lett* 2008;62:2143–5.
- [16] Coroller G, Lefeuvre A, Le Duigou A, Bourmaud A, Ausias G, Thierry Gaudry, et al. Effect of flax fibres individualisation on tensile failure of flax/epoxy unidirectional composite. *Compos A* 2013;51:62–70.
- [17] Schulte K. Damage development under cyclic loading. In: *Proceedings damage development and failure process in composite materials*, Leuven, Belgium, 04.–06.05; 1987.
- [18] Liu Q, Hughes M. The fracture behaviour and toughness of woven flax fibre reinforced epoxy composites. *Compos A* 2008;39:1644–52.
- [19] Varna J, Berglund LA. Thermo-elastic properties of composite laminates with transverse cracks. *J Compos Technol Res* 1994;16:77–87.
- [20] Gagel A, Lange D, Schulte K. On the relation between crack densities, stiffness degradation, and surface temperature distribution of tensile fatigue loaded glass-fibre non-crimp-fabric reinforced epoxy. *Compos A* 2006;37:222–8.
- [21] Joffe R, Varna J. Analytical modeling of stiffness reduction in symmetric and balanced laminates due to cracks in 90° layers. *Compos Sci Technol* 1999;59:1641–52.
- [22] Ogiyama S, Kobayashi S, Takeda N, Kobayashi A. Damage mechanics characterization of transverse cracking behavior in high-temperature CFRP laminates. *Compos Sci Technol* 2001;61:1049–55.

- [23] ISO 527-4, Determination of tensile properties-Test conditions for isotropic and orthotropic fibre-reinforced plastic composites. International Organization for Standardization; April 1997.
- [24] ISO 14126: 1999, Fibre-reinforced plastic composite - Determination of compressive properties in the in-plan direction. International Organization for Standardization; September 1999.
- [25] ISO 14129: 1997, Fibre-reinforced plastic composites - Determination of the in-plane shear stress/shear strain response, including the in-plane shear modulus and strength, by the  $\pm 45^\circ$  tension test method. International Organization for Standardization; December 1997.
- [26] Arbelaz A, Fernàndez B, Valea A, Mondragon I. Mechanical properties of short flax fibre bundle/poly(3-caprolactone) composites: Influence of matrix modification and fibre content. Carbohydr Polym 2006;64:224–32.
- [27] Bos HL, Donald AM. In situ ESEM study of the deformation of elementary flax fibres. J Mater Sci 1999;34:3029–34.
- [28] Grandidier JC, Casari P, Jochum C. A fibre direction compressive failure criterion for long fibre laminates at ply scale, including stacking sequence and laminate thickness effects. Compos Struct 2012;94:3799–806.